Journal of Power Sources 186 (2009) 278–285

Contents lists available at ScienceDirect

Journal of Power Sources

journal homepage: www.elsevier.com/locate/jpowsour

The diffusion overpotential increase and appearance of overlapping arcs on the Nyquist plots in the low humidity temperature test conditions of polymer electrolyte fuel cell

Soshin Nakamura [a], Hisao Nishikawa [a,*], Tsutomu Aoki [b], Yasuji Ogami [b]

[a] Department of Electrical Engineering, Tokyo Denki University, 2-2 Kandanishiki-cho, Chiyoda-ku, Tokyo 101-8457, Japan
[b] Fuel Cell Technology Development Department, Toshiba Fuel Cell Power System Corp, 4-1 Ukishima-cho, Kawasaki-ku, Kawasaki-shi, Kanagawa 210-0862, Japan

ARTICLE INFO

Article history:
Received 23 July 2008
Received in revised form 1 October 2008
Accepted 8 October 2008
Available online 17 October 2008

Keywords:
PEFC
AC impedance characteristics
Low relative humidity
Overpotential

ABSTRACT

We have investigated cell voltage characteristics and AC impedance characteristics of polymer electrolyte fuel cells (PEFCs) at various humidity temperatures for H_2/O_2 and H_2/air test conditions (current density: 200, 400, and 600 mA cm^{-2}, cell temperature: 80 °C, humidity temperature at respective electrodes: 40, 50, 60, and 70 °C). The diffusion overpotential increases with decreasing humidity in the low humidity temperature region such as 40 and 50 °C and the Nyquist plots obtained from AC impedance measurements show a small arc superposed on an elliptic arc in the low frequency region. The diameter of this small arc increases with decreasing humidity temperature from 50 to 40 °C or with increasing current density. These results suggest that oxygen transport across the ionomer film in the catalyst layer is significantly reduced in the low humidity condition, which causes a decrease in cell voltage, increase in diffusion overpotential, the appearance of overlapping arcs (two separate arcs) in the lower frequency region on the Nyquist plots, and the increase of mass transport resistance from Nyquist plots.

© 2008 Elsevier B.V. All rights reserved.

1. Introduction

Polymer electrolyte fuel cells (PEFCs) can operate at low temperatures and are suitable for fabrication of small light weight systems with high current density. Thus, there has been extensive developmental research into their use for residential and vehicular power. These fuel cells are, however, greatly affected by humidity. For instance, cell voltage is significantly reduced due to flooding in a high current density region. On the other hand, under low humidity conditions, although gas diffusivity is improved, cell resistance increases and catalyst activity is lowered due to water deficiency in the catalyst layer, and consequently cell voltage is lowered [1]. Continued operation at low humidity also causes cross-leak in membranes of MEA and degradation of membranes proceeds in a short time [2–4]. Under high humidity conditions, repeated application of voltage corresponding to the open circuit voltage (OCV) in the case of vehicle use causes sintering of the catalyst that decreases its surface area [5]. Humidity thus significantly affects performance as well as durability of the cells. In order to diagnose the cell voltage loss and cell degradation, we can use the cyclic voltammetry (CV) method to determine electrochemically the catalyst surface area, or the polarization loss method from the IR free cell voltage curve to examine the causes of cell voltage loss [6]. The electrochemical impedance spectroscopy method (AC impedance measurement method) is generally used for electrical characterization of electrochemical systems [7,8]. This method can supply information not only on cell resistance, but also on ionic conductivity in the catalyst layer, and gas diffusivity across the catalyst layer and gas diffusion layer (GDL). Thus, it is accepted as an important method for investigating the causes of cell voltage loss and cell degradation. Recently Xu et al. performed experiments on cell voltage loss in reduced humidity environments at high temperature (cell temperature: 120 °C, relative humidity: 20%) and shown that the observed significant decrease in cell voltage is due to oxygen transport loss across the ionomer film in the electrode [9]. On the other hand, using the AC impedance method Yan et al. have provided useful data on cell operating characteristics by determining charge transfer resistance and mass transfer resistance from the Nyquist plots for a 2-kW cell stack when quantitatively varying the relative humidity, flow rate and cell temperature [10].

In the present experiment, we have carried out H_2/O_2 and H_2/air tests at a cell temperature of 80 °C, variable humidity of fuel gas and oxidant, and determined the characteristics of cell voltage and AC impedance. In particular, as to the characteristics of cell voltage loss at low humidity operation, we have found an increase in diffusion overpotential even for low humidity conditions, and

* Corresponding author. Tel.: +81 3 5280 3692; fax: +81 3 5280 3687.
E-mail address: nishik@e.dendai.ac.jp (H. Nishikawa).

0378-7753/$ – see front matter © 2008 Elsevier B.V. All rights reserved.
doi:10.1016/j.jpowsour.2008.10.022

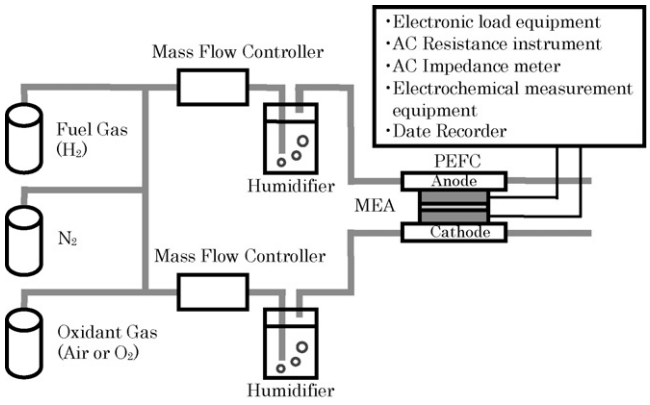

Fig. 1. Experiment equipment.

a phenomenon appearing on the Nyquist plots probably due to oxygen transport loss. These new findings on PEFC operating characteristics are reported in the following.

2. Experiment

The apparatus used in the present experiment is shown in Fig. 1 and the cell configuration is shown in Fig. 2. The reaction gas was controlled with a flow meter and introduced to a small single cell through a humidifier. MEA of 3 cm × 15 cm (PRIMEA® Series 5510, catalyst area: 45 cm^2, catalyst: 0.3 mg cm^{-2}, membrane: Gore-select® 30 μm, GDL: Carbel®-CFP200) from Gore Co. Ltd. was used as the cell. The carbon separator had 16 straight flow paths (length: 150 mm, rib width: 1 mm, channel width: 1 mm, and channel depth: 0.5 mm on cathode side and 0.4 mm on anode side) and counter flow was used for fuel and oxidant gas flow. In H_2/O_2 tests, the flow rate was set for hydrogen utilization of 70% and oxygen utilization of 8.4%, and in the H_2/air tests, hydrogen utilization of 70% and air utilization of 40%. Cell temperature was 80 °C, humidity temperatures for cathode/anode were 40/40, 50/50, 60/60 and 70/70 °C and current density was 200, 400, and 600 mA cm^{-2}. Cell resistance was measured with a low-resistance meter, Tsuruga Electric Co. (MODEL 3566), and AC impedance with an instrument from NF Electronic Instruments (5080 FRA) applying an alternate current of 10% amplitude to the single cell current within a frequency range from 20 kHz to 0.01 Hz.

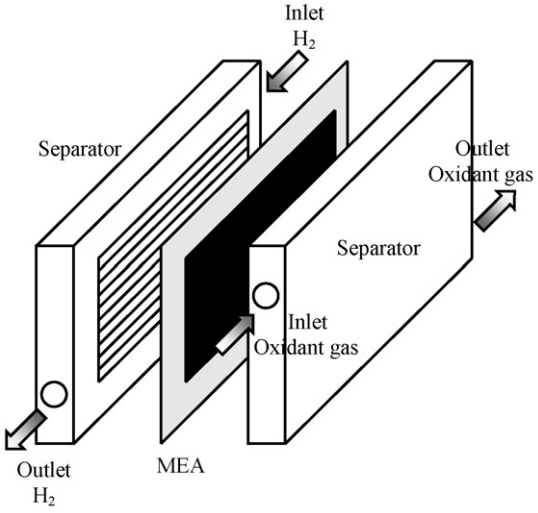

Fig. 2. Cell configuration.

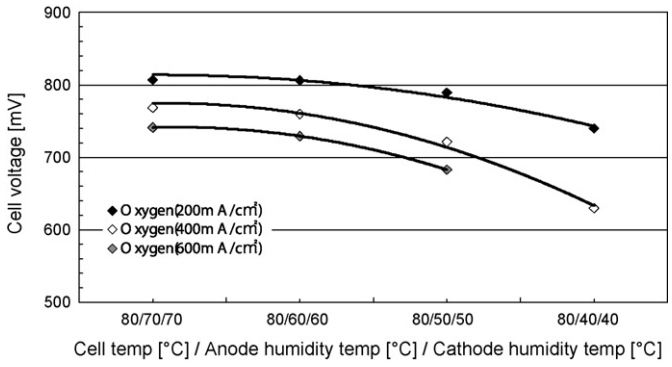

Fig. 3. Cell voltage characteristic of H_2/O_2 tests.

3. Results

3.1. Results for H_2/O_2 tests

Fig. 3 shows cell voltage characteristics for various humidity temperatures. With decreasing humidity temperature, cell voltage decreases gradually. The cell voltage decreases for a humidity temperature of 40 °C at current density 400 mA cm^{-2}. The test could not be made at 600 mA cm^{-2}. Results of the Nyquist plots obtained from AC impedance measurements are shown in Fig. 4. At humidity temperature of 60 °C and more, elliptic arcs were obtained for all current densities. At humidity temperature of 50 °C, an arc, with another smaller arc superposed at low frequency, was observed at high current density (400 mA cm^{-2}). At humidity temperature of 40 °C, overlapping arcs with another smaller arc superposed were observed at current density 200 mA cm^{-2}. With increasing current density the diameter of the arc in the higher frequency region (the first arc) decreases and in the lower frequency region the diameter of the second arc increases.

3.2. Results for H_2/air tests

I–V characteristics for H_2/air tests are given in Fig. 5. At humidity temperature of 70 °C, cell voltage loss increases with increasing current density, and more significantly than in the case of H_2/O_2 tests. Cell voltage reduction is large even in the low humidification region such as at 40 °C. The Nyquist plots are shown in Fig. 6. Due to gas diffusion blocking at humidity temperature of 70 °C, a rather large arc is obtained at 600 mA cm^{-2}, in contrast with the case of H_2/O_2 tests, which show a decrease in arc diameter with increasing current density. At 60 °C a distorted elliptic arc is obtained. At 50 and 40 °C, a second arc is superposed on the first arc in the low frequency region, similar to the phenomena found for H_2/O_2 tests. With increasing current density the diameter of the first arc becomes smaller, while that of the second arc increases, similar to the observation for H_2/O_2 tests.

4. Discussion

4.1. Polarization loss

We have investigated the factors involved in cell voltage losses when varying the humidity temperature. Fig. 7 shows the results obtained from measurements of cell resistance with a low-resistance meter, and impedance spectroscopy for various humidity temperatures and current densities. Cell resistance represents the

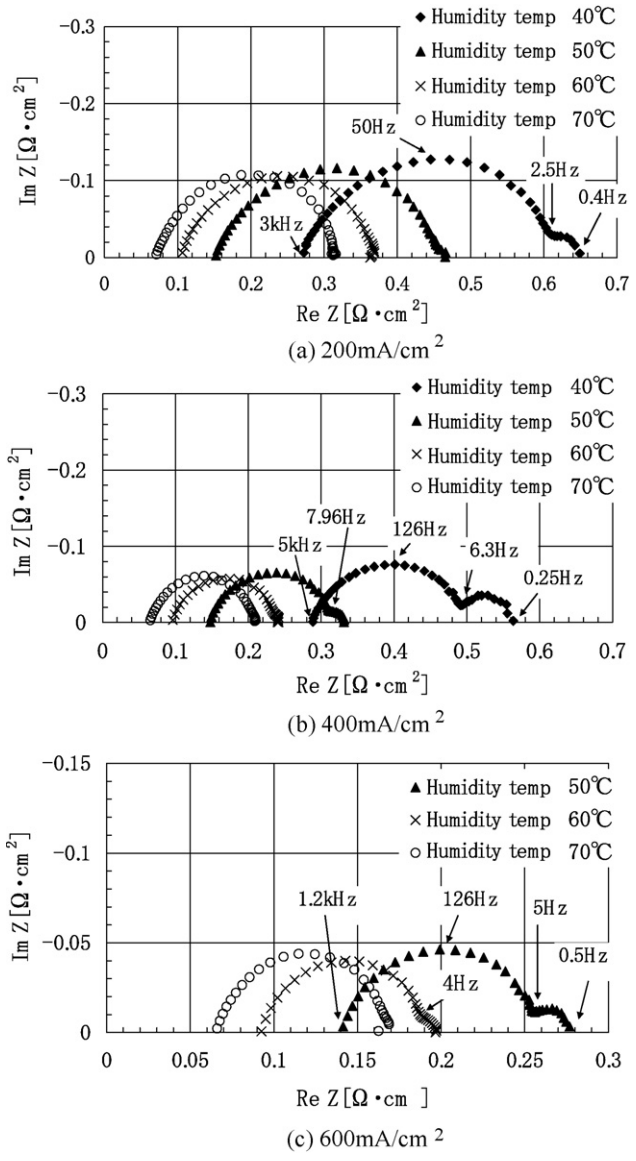

Fig. 4. Nyquist plots for various humidity temperatures for H_2/O_2 tests: (a) 200 mA cm^{-2}, (b) 400 mA cm^{-2} and (c) 600 mA cm^{-2}.

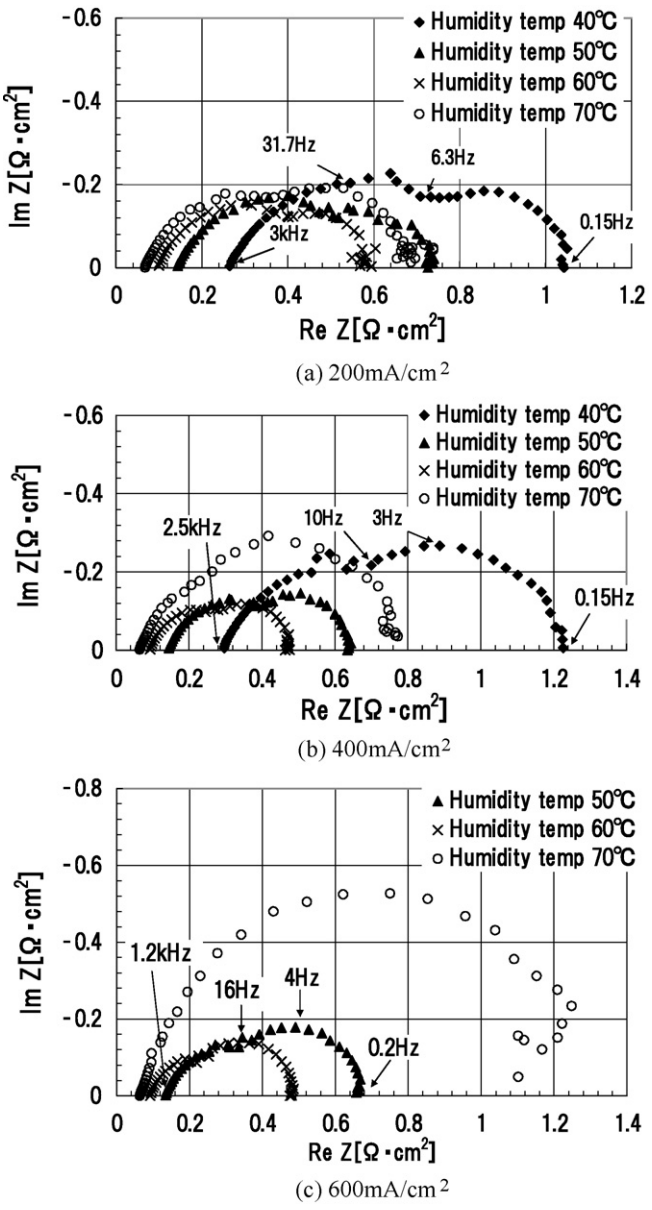

Fig. 6. Nyquist plots of various humidity temperatures for H_2/air tests: (a) 200 mA cm^{-2}, (b) 400 mA cm^{-2} and (c) 600 mA cm^{-2}.

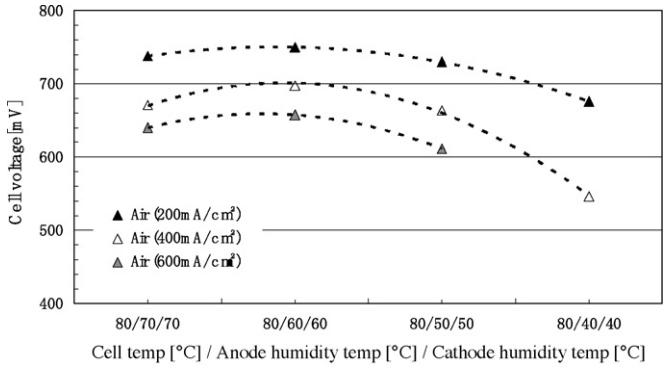

Fig. 5. Cell voltage characteristic of H_2/air tests.

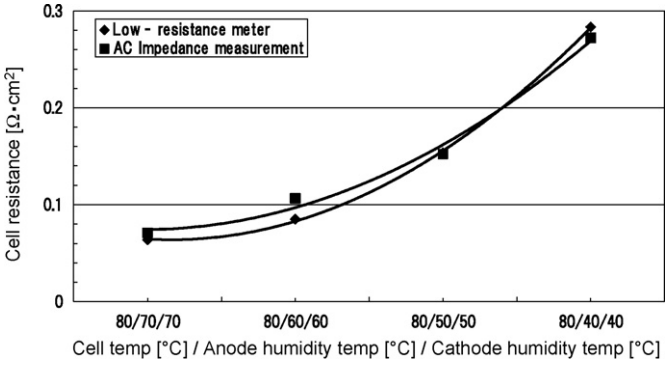

Fig. 7. Comparison of cell resistance (low-resistance meter method and AC impedance measurement method).

total ohmic resistance of the cell, which can be expressed as the sum of the contributions from contact resistance between components and ohmic resistance of the cell components such as the membrane, catalyst layer, gas diffusion layer and bipolar plates. A low-resistance meter is used at 1 kHz of AC frequency. In the case of AC impedance spectrum the high frequency (about 1–5 kHz) intercept part (intersection with the real axis in impedance spectrum) reflects the ohmic resistance of the cell. Cell resistances from the low-resistance meter and AC impedance measurements are in fair agreement and increase with decreasing humidity temperature. So using this AC impedance measurement resistance, IR free *I–V* characteristics are obtained, from which overpotential was determined for each current density. The standard voltage for the polarization curves was set at 900 mV, and the Tafel slope was determined in the low current density region. Then activation overpotential was calculated from Eq. (1), diffusion overpotential from Eq. (2) and resistance overpotential from Eq. (3), respectively,

$$\eta_{\text{act}} = b \log\left(\frac{i}{i_{0.9}}\right) \quad (1)$$

$$\eta_{\text{diff}} = 900 - V - (\eta_{\text{act}} + \eta_{\text{r}}) \quad (2)$$

$$\eta_{\text{r}} = ir \quad (3)$$

where r is the cell resistance ($\Omega\,\text{cm}^2$), i is the observed current density (mA cm^{-2}), V is the observed cell voltage (mV), b is the Tafel slope (mV decade^{-1}), and $i_{0.9}$ is the current density (mA cm^{-2}) at 0.9 V.

4.1.1. Overpotential for H_2/O_2 tests

Overpotential (H_2/O_2) test results are shown in Fig. 8. Activation overpotential increases almost linearly with decreasing humidity temperature. With decreasing humidity temperature, water content in the cell decreases, and consequently water in the catalyst layer decreases to reduce ionic conductivity of ionomer in the catalyst layer. The catalyst utilization decreases due to the shortage of active catalyst area, which presumably causes an increase in activation overpotential. Diffusion overpotential shows a small increase at the high humidity temperature of 70 °C and at the low humidity temperature of 40 °C a slight increase in diffusion overpotential was observed. The reason for this will be discussed later. Resistance overpotential increases with decreasing humidity temperature.

4.1.2. Overpotential for H_2/air tests

Overpotential (H_2/air) test results are shown in Fig. 9. The activation overpotential increases with decreasing humidity temperature. This is similar to that found for H_2/O_2 tests. The increase in activation overpotential is larger than that in the H_2/O_2 tests due to a lower oxygen concentration. A considerable difference from the results for H_2/O_2 tests is found in the variation of diffusion overpotential. In the high humidity region of 70 °C, a large diffusion overpotential was observed because gas diffusion blocking may take place due to an excess of water in GDL and catalyst layer. On the other hand at 40 °C, large diffusion overpotential was observed. Generally speaking, water content in the GDL and catalyst layer will decrease with decreasing humidity temperature so that diffusion loss will be reduced. But this time overpotential increased. This is based on another factor of diffusion loss. This will be discussed later.

4.2. Nyquist plots

Nyquist plots of H_2/O_2 test are shown in Fig. 4. The diameter of the kinetic loop decreases with humidity temperature increase, and the current increases because the water content in the cell increases with the humidity temperature and the current increase. On the other hand, a small arc is found superposing on a large arc at the lower frequency in the Nyquist plots and begins to grow at current density 400 mA cm^{-2} for humidity temperature 50 °C and the current density 200 mA cm^{-2} for humidity temperature 40 °C. This may be the same phenomenon associated with the large diffusion overpotential observed at humidity temperature 40 °C. This reason will be discussed later.

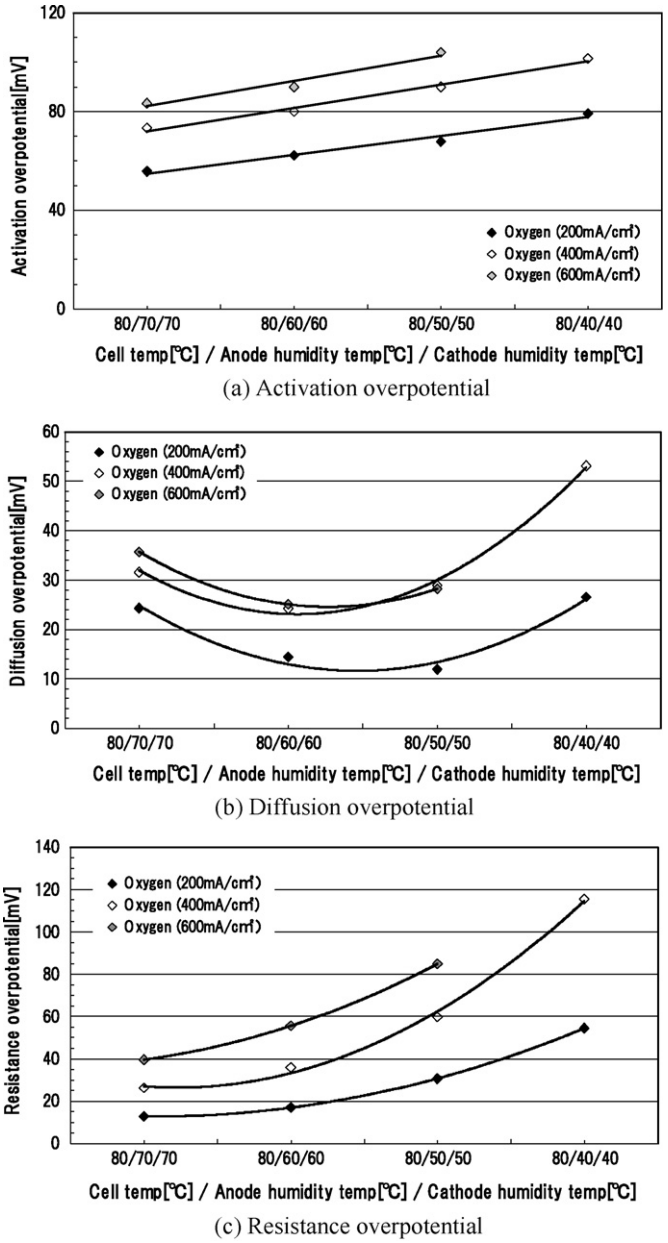

Fig. 8. Polarization loss for H_2/O_2 tests: (a) activation overpotential, (b) diffusion overpotential and (c) resistance overpotential.

Nyquist plots of H_2/air test are shown in Fig. 6. The diameter of the two overlapping arcs is very large at the test condition of current density 600 mA cm^{-2} and humidity temperature 70 °C. This may be due to gas diffusion blocking generation in the GDL and catalyst layer. The diameter of the two overlapping arcs decreases with humidity temperature, and current decreases because the water content in the cell decreases and limits mass transfer. On the other hand, the low frequency arc begins to grow at humidity temperature of 50 and 40 °C the same as in the H_2/O_2 test. The diameter of arc increases with humidity temperature decrease and current

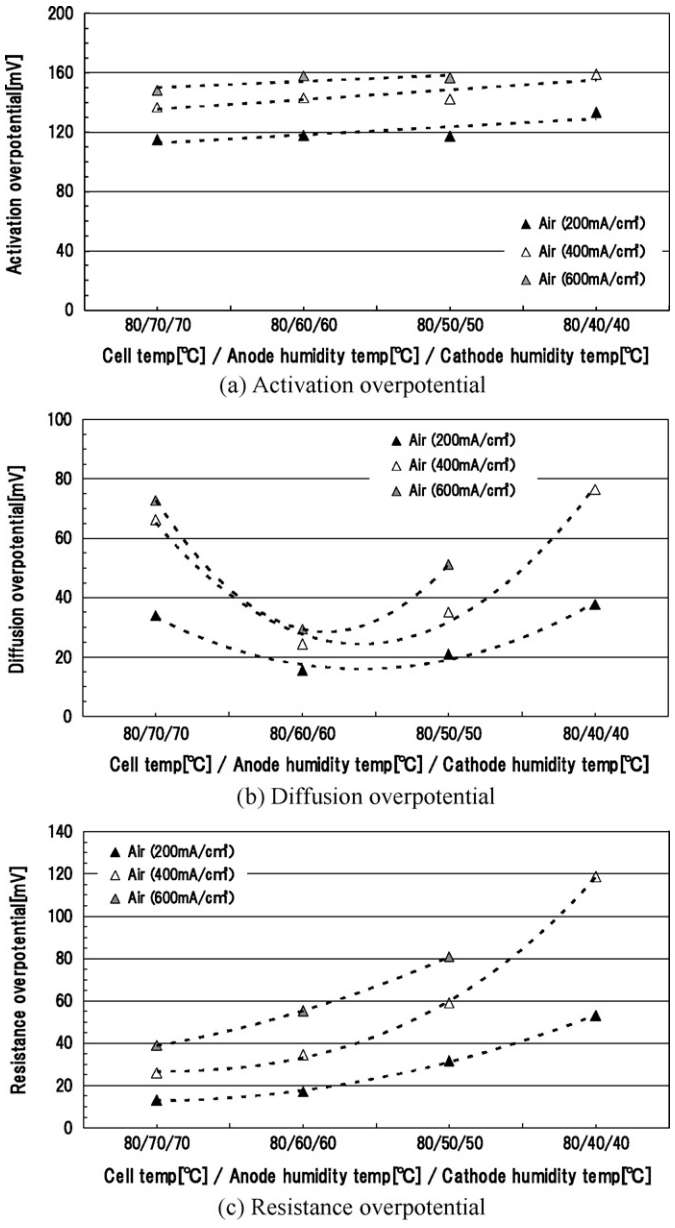

Fig. 9. Polarization loss for H_2/air tests: (a) activation overpotential, (b) diffusion overpotential and (c) resistance overpotential.

density increase and is large compared with the H_2/O_2 test. The reason for this will be discussed later.

4.3. Charge transfer resistance and mass transfer resistance from Nyquist plots

The equivalent circuit for AC impedance analysis is shown in Fig. 10(a) [10]. The high frequency intercept reflects the real ohmic resistance (R_{ohm}) of a single cell. R_{ct} is the charge transfer resistance due to the oxygen reduction reaction and relative humidity and double layer capacitance (CPE_1) within the catalyst layer. R_{mt} is the mass transfer resistance of oxygen in the catalyst and gas diffusion layer. So CPE_2 is considered to be the associated constant phase. We intend to measure the impedance at low overpotential with pure hydrogen for the anode to minimize the anode effect such as CO poisoning, NH_3 contamination and H_2S contamination. So that anode impedance is very small due to the fast hydrogen oxidation and therefore can be neglected. The measured electrochemical impedance is fitted using our software [11]. The AC impedance spectrum and its fitted curve are shown in Fig. 10(b). The fitted curve is in good agreement with the measurements. This shows that the electrochemical processes of a single cell can be analyzed by our software. The relation between charge transfer resistance and humidity temperature is shown in Fig. 11(a) for various current density. As the humidity temperature decreases, the charge transfer resistance increases and gradually decreases with increas-

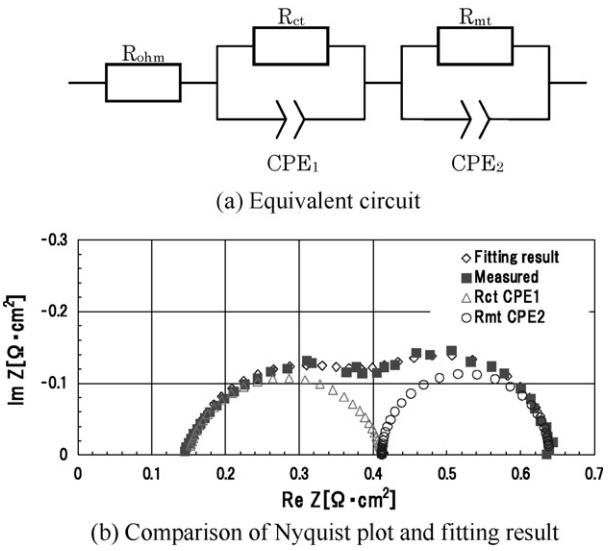

Fig. 10. Curve fitting: (a) equivalent circuit and (b) comparison of Nyquist plot and fitting result.

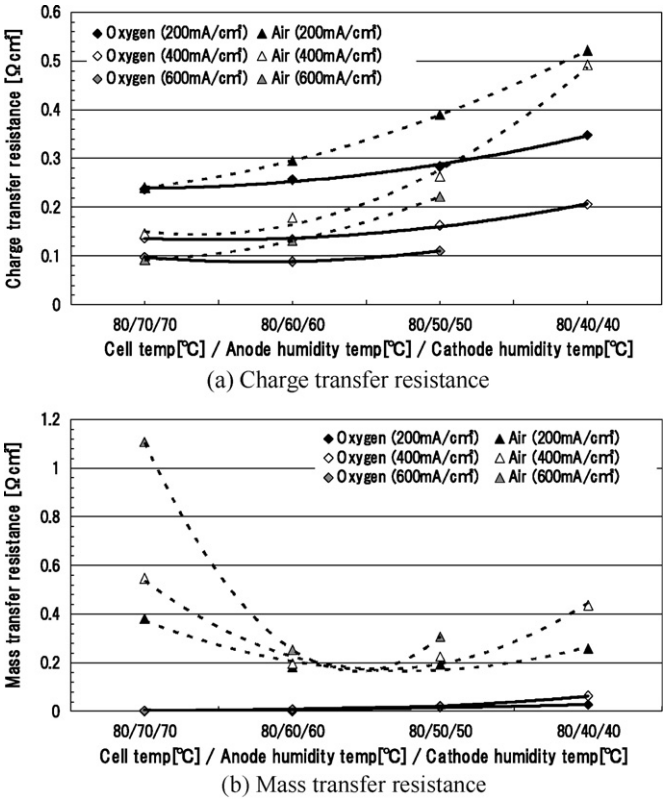

Fig. 11. Curve fitting results: (a) charge transfer resistance and (b) mass transfer resistance.

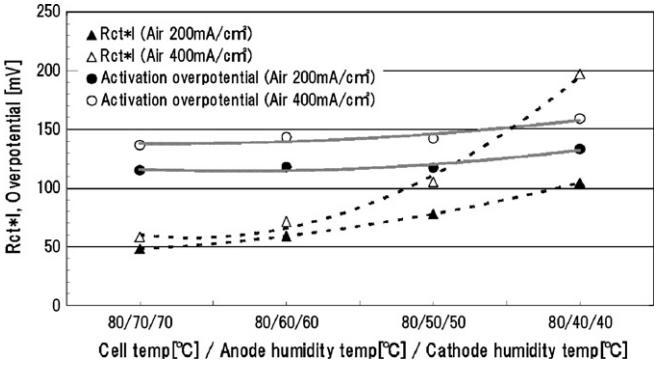

Fig. 12. Relationship between $R_{ct}I$ and activation overpotential for H_2/air test.

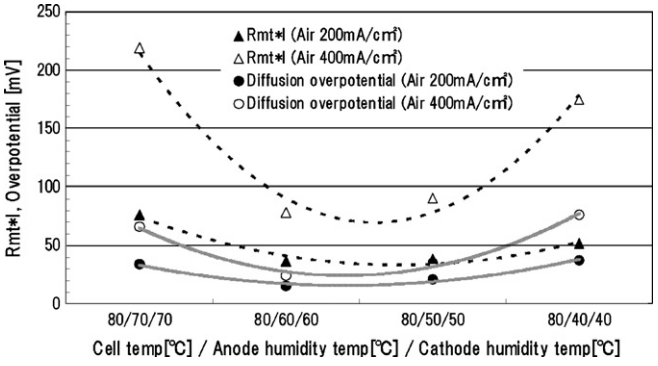

Fig. 13. Relationship between $R_{mt}I$ and diffusion overpotential for H_2/air test.

ing current density. The reason for the increasing resistance is that water content in the cell is less as humidity temperature decreases, leading to lower ion conductivity in the catalyst layer and decreasing the catalyst utilization. On the other hand, the water generated in the cell will be increased with increasing current density, thus charge transfer resistance will decrease. The charge transfer resistance in H_2/air test is larger than that in H_2/O_2 test, because catalyst activity depends on oxygen concentration in the cell and oxygen concentration is smaller than that in H_2/O_2 test.

The relation between mass transport resistance and humidity temperature is shown in Fig. 11(b). In the high humidity temperature region the mass transport resistance gradually decreases with decreasing humidity temperature, but after the humidity temperature declines to a value of about 50 °C, the mass transport resistance (R_{mt}) begins to increase as the humidity temperature decreases. Also R_{mt} increases with increasing current density. Because water generated in the cell will increase with increasing current density, the higher water level can block oxygen transport because of the amount of water in the gas diffusion layer. This leads to an increase in mass transport resistance. As humidity temperature decreases in the high humidity temperature region, water content in the catalyst layer and gas diffusion decreases, thus oxygen gas transport through these layers will increase, which leads to a decrease in mass transport resistance. When humidity temperature is 40–50 °C, conventional gas diffusion blocking may not occur due to less water content in the catalyst layer and gas diffusion layer. However in the lower humidity temperature region, mass transfer resistance increases with decreasing humidity temperature. This reason is discussed later.

4.4. Relation between overpotential from I–V characteristics and $R_{ct}I$, $R_{mt}I$

We derived the overpotential from the *I–V* characteristics curve in Section 4.1 and charge transfer resistance (R_{ct}) and mass transfer resistance (R_{mt}) from the Nyquist plots in Section 4.3. Resistive overpotential is given by Eq. (3). So we took $R_{ct}I$ as an estimated activation loss and $R_{mt}I$ as an estimated diffusion loss. The relation between activation overpotential and $R_{ct}I$ is shown in Fig. 12 and the relation between diffusion overpotential and $R_{mt}I$ is shown in Fig. 13 both for various humidity temperatures and current densities. Because charge transfer resistance and mass transfer resistance in H_2/air test is larger than that in H_2/O_2 test, we compared overpotential and $R_{ct}I$, $R_{mt}I$ at H_2/air test conditions. The activation and diffusion overpotential values from *I–V* characteristics are different from $R_{ct}I$ and $R_{mt}I$, so we cannot estimate activation and diffusion overpotential values from $R_{ct}I$ and $R_{mt}I$. But we are able to estimate from AC impedance analysis and Nyquist plots, for example, that the increase in charge transfer resistance indicates a decrease in ion conductivity in the ionomer in the catalyst, i.e. the lowering of the catalyst utilization and the increase of the mass transfer resistance indicates increasing gas diffusion blocking when varying the humidity temperature and the current density.

4.5. Effect of oxygen concentration on activation overpotential

We conducted H_2/O_2 test and H_2/air test to investigate the effect of oxygen concentration. Activation overpotential and difference of activation overpotential in H_2/O_2 and H_2/air test are shown in Fig. 14 for various humidity temperatures at a current density of 200 mA cm^{-2}. The difference in the activation overpotential between H_2/O_2 and H_2/air test is estimated to be 50–60 mV. We can calculate the difference in activation overpotential for the H_2/O_2 and H_2/air test from Eq. (4) [12] and evaluated the effect of oxygen concentration for activation overpotential.

$$\Delta E = E_{O_2} - E_{air} = 2.303\left(\frac{RT}{F}\right)\log\left(\frac{P_{O_2}}{P_{air}}\right) \quad (4)$$

where R is the universal gas constant (J (mol K)$^{-1}$), T is the absolute cell temperature (K), F is the Faraday constant (C mol^{-1}), P_{O_2} is the partial pressure of oxygen (atm), and P_{air} is the partial pressure of oxygen in air (atm).

Since P_{O_2} and P_{air} in Eq. (4) depend on the relative humidity in the cell, we measured the water content of the exhausted air at the current density 200 mA cm^{-2} while changing the humidity temperature from 50 to 60 to 70 °C and derived the average relative humidity in the cell from the inlet and outlet water content in the air flow and estimated the partial pressure of oxygen and partial pressure of oxygen in air in the H_2/O_2 and H_2/air tests. These partial pressures are shown in Fig. 15. We calculated the difference in activation overpotential for the H_2/O_2 and H_2/air test from Eq. (4) using the test results and show the calculation and measurement results

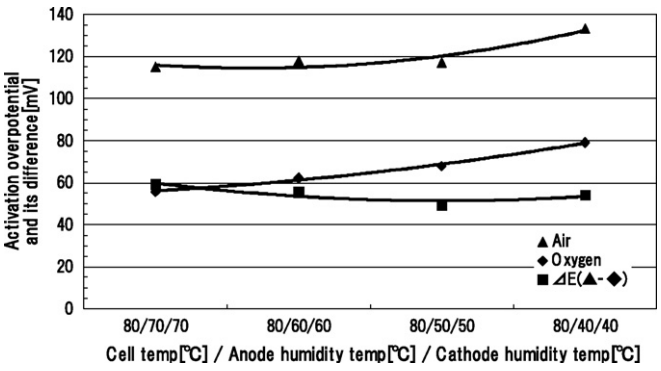

Fig. 14. Activation overpotential in H_2/O_2 and H_2/air test and its difference.

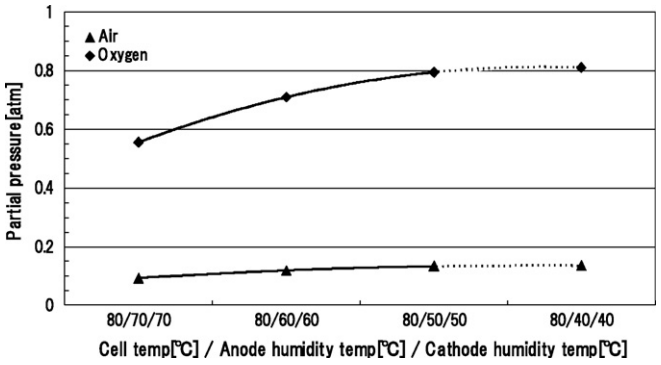

Fig. 15. Calculation result for partial pressure.

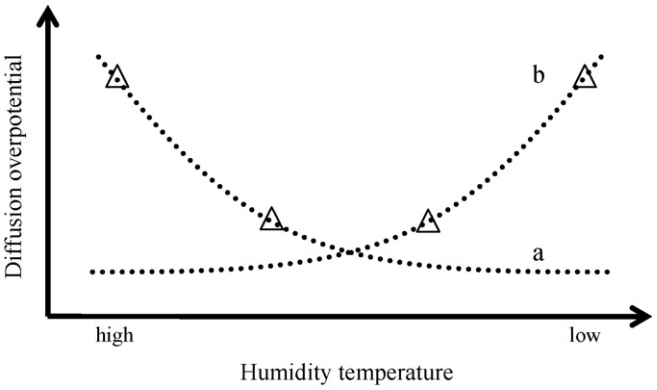

Fig. 17. Relation between humidity temperature and diffusion overpotential.

in Fig. 16. Fig. 16 shows fair agreement between the calculated and measured results. This means that the difference in activation overpotential in the H_2/O_2 and H_2/air tests is derived from the partial pressure of oxygen based on the relative humidity in the cell.

4.6. Cause of cell voltage loss

4.6.1. Cell voltage loss due to gas diffusion blocking

In H_2/O_2 tests at a humidity temperature of 70 °C, arcs of the Nyquist plots are elliptic and their diameter decreases with increasing current density as shown in Fig. 4. This causes an increase in water content in the catalyst layer to promote its catalyst activity. No sign of gas diffusion blocking is found since pure oxygen is supplied even at high humidity conditions. On the other hand, in H_2/air tests, gas diffusion blocking takes place as current density increases and the Nyquist plots show large overlapping arcs probably due to the interference of gas diffusion. With decreasing current density, the diameter of the second of the overlapping arcs becomes smaller and the superposition point of the two overlapping arcs shifts to the lower frequency region. As shown in Fig. 8, the diffusion overpotential in H_2/O_2 tests at 70 °C humidification increases slightly compared to that at 60 °C in spite of single arcs in Nyquist plots for all current densities, while in H_2/air tests the diffusion overpotential increases significantly as shown in Fig. 9. This is in accord with the two overlapping large arcs found on the Nyquist plots. The increase in diffusion overpotential, the observations of overlapping arcs and the increase of mass transfer resistance in higher humidity temperature especially in H_2/air test may indicate that gas diffusivity is interfered with by water present in pores in the GDL and catalyst layer.

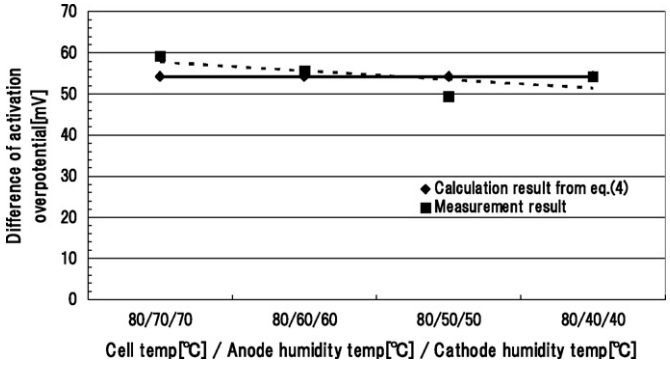

Fig. 16. Comparison of calculation and measurement results for difference of activation overpotential in H_2/O_2 and H_2/air test.

4.6.2. Cell voltage loss due to decrease of catalyst utilization

The amount of water supplied to the cell decreases with decreasing humidity temperature, which causes an increase in cell resistance as well as a decrease in proton conductivity through the ionomer in the catalyst layer. As a result, the catalyst utilization decreases and consequently the catalyst activity and cell voltage are reduced. As shown in Figs. 8(a), 9(a) and 11(a), the activation overpotential and charge transfer resistance for H_2/O_2 and H_2/air tests increase with decreasing humidity temperature. Also as the water content in the cell decreases with decreasing humidity temperature, gas diffusivity increases, so that diffusion overpotential decreases. As cell voltage is determined from the difference between the activation overpotential increase and the diffusion overpotential decrease when decreasing humidity temperature, maximum cell voltage was observed especially at humidity temperature 60 °C in the H_2/air test as shown in Fig. 5.

4.6.3. Cell voltage loss due to oxygen transport loss across the ionomer film in the catalyst layer

Figs. 8(b) and 9(b) show that diffusion overpotential increases for the higher and lower humidity temperatures. From this test result the diffusion overpotential increase depends on two different factors, one is the interference of gas diffusion due to water content increase in the GDL and catalyst layer at the higher humidity temperature and the other is the oxygen transport loss across the ionomer film in the catalyst layer due to the water content decrease in the catalyst layer at the lower humidity temperature. Fig. 17 shows curve 'a' which is the diffusion loss due to the interference of gas diffusion which decreases with humidity temperature decreasing, and curve 'b' is the diffusion loss due to the oxygen transport loss across the ionomer film which increases with decreasing humidity temperature as pointed out by Xu et al. [9]. The ionomer in the catalyst layer must have sufficient oxygen permeability so that the oxygen across it proceeds without mass transfer losses at the higher humidity condition. But we expect it to be difficult to transport oxygen across the ionomer film at the lower humidity condition as well as the crossover decrease of H_2 and O_2 through the membrane with decreasing humidity temperature [13]. As shown in Fig. 4 in H_2/O_2 tests a small arc is found superposed on a larger arc in the lower frequency region on the Nyquist plot for current density larger than 400 mA cm^{-2} at humidity temperature of 50 °C. Lowering the humidity temperature to 40 °C, this small arc is found even for a current densities of 200 mA cm^{-2}. Thus the diameter of the superposed arcs increases with decreasing humidity temperature and increasing current density. Similar to H_2/O_2 tests, overlapping arcs are also observed in H_2/air tests at a humidity temperature of 40 and 50 °C as shown in Fig. 6. In this case the diameter of the second arc is larger than that in the case of

the H_2/O_2 test due to oxygen concentration lowering. These results suggest that oxygen transport across the ionomer film in the catalyst layer is significantly reduced for the low humidity condition, which causes a decrease in cell voltage, increase in diffusion overpotential, the appearance of overlapping arcs (two separate arcs) in the lower frequency region on the Nyquist plots, and the increase of mass transport resistance from Nyquist plots.

5. Conclusions

We have investigated the cell voltage characteristics and AC impedance characteristics of PEFCs at various humidity temperatures for H_2/O_2 and H_2/air tests. The results are as follows:

(1) The activation overpotential obtained from IR free voltage curves for H_2/O_2 and H_2/air tests increases almost linearly with decreasing humidity temperature. This is because the proton conductivity through the ionomer in the catalyst layer decreases due to the decrease in water content in the catalyst layer with decreasing humidity temperature, which causes a decrease in catalyst utilization and catalyst activity, and consequently a decrease in cell voltage. The diameter of arcs on the Nyquist plots increases with decreasing humidity temperature, reflecting the decrease in catalyst utilization.

On the other hand, the diffusion overpotential shows a minimum at 60 °C and increases at 70, 50 and 40 °C. This tendency is more obvious for H_2/air tests, and gas diffusion blocking is observed on the Nyquist plots for a humidity temperature of 70 °C. And it was found that diffusion overpotential increases with reducing humidity in the region of low humidity temperatures such as 40 and 50 °C.

(2) We derived the charge transfer resistance (R_{ct}) and mass transport resistance (R_{mt}) from Nyquist plots. The charge transfer resistance increases with decreasing humidity temperature and gradually decreases with increasing current density. This is because the water content in the cell will be less with a decrease in humidity temperature, leading to lowering the ion conductivity in the catalyst layer and decreasing catalyst utilization. On the other hand, water in the cell will increase with increasing current density, thus charge transfer resistance will decrease.

In the high humidity temperature region mass transport resistance gradually decreases with decreasing humidity temperature, but after the humidity temperature declines to a value of about 50 °C, the mass transfer resistance begins to increase as the humidity temperature decreases. In the higher humidity temperature region, conventional gas diffusion blocking may occur and in the lower humidity temperature region gas diffusion blocking may occur due to another factor, i.e. oxygen transport reduction across the ionomer film in the catalyst layer.

(3) Resistive overpotential is given by Eq. (3). So we took $R_{ct}I$ as an estimated activation loss and $R_{mt}I$ as an estimated diffusion loss. We compared the overpotential and $R_{ct}I$, $R_{mt}I$ for H_2/air tests. As a result we found that activation and diffusion overpotential values from I–V characteristics are different from $R_{ct}I$ and $R_{mt}I$ and so we cannot estimate activation and diffusion overpotential values from $R_{ct}I$ and $R_{mt}I$. But we are able to estimate from AC impedance analysis and Nyquist plots, for example, that the increasing charge transfer resistance indicates a decrease in the ion conductivity in the ionomer in the catalyst, i.e. a lowering of the catalyst utilization and an increase in the mass transfer resistance indicates an increasing gas diffusion blocking when varying the humidity temperature and the current density.

(4) We took that the difference of activation overpotential in H_2/O_2 and H_2/air test depends on the partial pressure of oxygen and the partial pressure of oxygen in air based on the relative humidity in the cell. The calculated result from Eq. (4) and the measured result are in fair agreement.

(5) Diffusion overpotential increases were observed in the higher (70 °C) and lower humidity temperature (50 and 40 °C) regions when changing the humidity temperature. Especially we found that diffusion overpotential increases with reduced humidity in the region of low humidity temperature such as 40 and 50 °C and that the Nyquist plots obtained from AC impedance measurements show a small arc superposed on an elliptic arc in the low frequency region. The diameter of this small arc increases with decreasing humidity temperature from 50 to 40 °C or with increasing current density. From these results it appears that oxygen transport across the ionomer film in the catalyst layer is significantly reduced at the low humidity condition, which causes a decrease in cell voltage, increase in diffusion overpotential, the appearance of overlapping arcs (two separate arcs) in the lower frequency region on the Nyquist plots, and the increase of mass transport resistance from Nyquist plots.

References

[1] H. Nishikawa, T. Sugawara, R. Kurihara, T. Aoki, Y. Ogami, Transactions of the Institute of Electrical Engineers of Japan B 125 (7) (2005) 680–686 (in Japanese).
[2] M. Hori, J. Yu, K. Kobayashi, M. Kato, The 12th FCDIC Symposium Proceedings, 2005, pp. 89–92 (in Japanese).
[3] E. Endoh, S. Terazono, H. Widjaja, Y. Takimoto, Electrochemical and Solid-State Letters 7 (7) (2004) A209–A211.
[4] M. Inaba, R. Umebayashi, M. Sugushita, H. Yamada, J. Tominaga, A. Tasaka, The 13th FCDIC Symposium Proceedings, 2006, pp. 86–89 (in Japanese).
[5] J. Xie, D.L. Wood, K.K. More, P. Atanassov, R.L. Borup, Journal of The Electrochemical Society 152 (5) (2005) A1011–A1020.
[6] H.A. Gasteiger, W. Gu, R. Makharia, M.F. Mathias, B. Sompalli, Handbook of Fuel Cells, vol. 3, John Wiley and Sons, 2003.
[7] N. Fouquet, C. Doulet, C. Nouillant, G. Dauphin-Tanguy, B. Ould-Bouamama, Journal of Power Sources 159 (2006) 905–913.
[8] X. Yuan, H. Wang, J.C. Sun, J. Zhang, International Journal of Hydrogen Energy 32 (2007) 4365–4380.
[9] H. Xu, H. Russell Kunz, J.M. Fenton, Electrochimica Acta 52 (2007) 3525–3533.
[10] X. Yan, M. Hou, L. Sun, D. Liang, Q. Shen, H. Xu, P. Ming, B. Yi, International Journal of Hydrogen Energy 32 (2007) 4364–4368.
[11] M. Itagaki, H. Hasegawa, K. Watanabe, T. Hachiya, Electrochemistry 72 (8) (2004) 550–556 (in Japanese).
[12] S.S. Kocha, Handbook of Fuel Cells, vol. 3, John Wiley and Sons, 2003.
[13] H.A. Gasteiger, M.F. Mathias, General Motors Corporation-Fuel Cell Activities, Proceedings of the Third International Symposium on Proton Conducting Membrane Fuel Cells, 202nd Meeting of the ECS, Salt Lake City, October 2002 (can be downloaded at http://www. engr. uconn. edu/~jmfent/Mark Mathias GM paper.pdf).